

A comprehensive progenitor model for SNe Ia

X. Meng and W. Yang

School of Physics and Chemistry, Henan Polytechnic University, Jiaozuo, 454000, China

`xiangcunmeng@hotmail.com`

ABSTRACT

Although the nature of the progenitor of Type Ia supernovae (SNe Ia) is still unclear, the single-degenerate (SD) channel for the progenitor is currently accepted, in which a carbon-oxygen white dwarf (CO WD) accretes hydrogen-rich material from its companion, increases its mass to the Chandrasekhar mass limit, and then explodes as a SN Ia. The companion may be a main sequence or a slightly evolved star (WD + MS), or a red-giant star (WD + RG). Incorporating the effect of mass-stripping and accretion-disk instability on the evolution of WD binary, we carried out binary stellar evolution calculations for more than 1600 close WD binaries. As a result, the initial parameter spaces for SNe Ia are presented in an orbital period-secondary mass ($\log P_1, M_2^1$) plane. We confirmed that in a WD + MS system, the initial companion leading to SNe Ia may have mass from $1 M_\odot$ to $5 M_\odot$. The initial WD mass for SNe Ia from WD + MS channel is as low as $0.565 M_\odot$, while the lowest WD mass from the WD + RG channel is $1.0 M_\odot$. Adopting the results above, we studied the birth rate of SNe Ia via a binary population synthesis approach. We found that the Galactic SNe Ia birth rate from SD model is $2.55 - 2.9 \times 10^{-3} \text{ yr}^{-1}$ (including WD + He star channel), which is slightly smaller than that from observation. If a single starburst is assumed, the distribution of the delay time of SNe Ia from the SD model may be a weak bimodality, where WD + He channel contributes to SNe Ia with delay time shorter than 10^8 yr and WD + RG channel to those with age longer than 6 Gyr.

Subject headings: binaries: close - stars: evolution - stars: dwarf novae - supernovae: general - white dwarfs

1. INTRODUCTION

1.1. Progenitor Models

Type Ia supernovae (SNe Ia) play an important role in astrophysics, especially in cosmology. They appear to be good cosmological distance indicators and are successfully applied in determining cosmological parameters (e.g. Ω and Λ), which leads to the discovery of the accelerating expansion of the universe (Riess et al. 1998; Perlmutter et al. 1999). At present, SNe Ia are proposed to be cosmological probes for testing the evolution of the Dark Energy equation of state with time (Howell et al. 2009a). However, the progenitor systems of SNe Ia have not yet been confidently identified (Hillebrandt & Niemeyer 2000; Leibundgut 2000), although they show their im-

portance in many astrophysical field, e.g. determining cosmological parameters, studying galaxy evolution, understanding explosion mechanism of SNe Ia and constraining the theory of binary stellar evolution (see the review by Livio 1999).

There is a consensus that SNe Ia result from the explosion of a carbon-oxygen white dwarf in a binary system (Hoyle & Fowler 1960). The CO WD accretes material from its companion, increases mass to its maximum stable mass, and then explodes as a thermonuclear runaway. Almost half of the WD mass is converted into radioactive nickel-56 in the explosion (Branch 2004), and the amount of nickel-56 determines the maximum luminosity of SNe Ia (Arnett 1982). According to the nature of the companions of the mass accreting white dwarfs, two basic scenarios for the progenitor of SN Ia have been dis-

cussed over the last three decades. One is the single degenerate (SD) model (Whelan & Iben 1973; Nomoto, Thielemann & Yokoi 1984), in which a CO WD increases its mass by accreting hydrogen- or helium-rich matter from its companion, and explodes when its mass approaches the Chandrasekhar mass limit. The companion may be a main-sequence or a slightly evolved star (WD+MS) or a red-giant star (WD+RG) or a helium star (WD + He star) (Yungelson et al. 1995; Li & van den Heuvel 1997; Hachisu et al. 1999a,b; Nomoto et al. 1999, 2003; Langer et al. 2000; Han & Podsiadlowski 2004, 2006; Chen & Li 2007, 2009; Han 2008; Meng, Chen & Han 2009; Meng & Yang 2009; Lü et al. 2009; Wang et al. 2009a,b). An alternative is the double degenerate (DD) model (Iben & Tutukov 1984; Webbink 1984), in which a system consisting of two CO WDs loses orbital angular momentum by gravitational wave radiation and merges finally. The merger may explode if the total mass of the system exceeds the Chandrasekhar mass limit (see the reviews by Hillebrandt & Niemeyer 2000 and Leibundgut 2000). Although the channel is theoretically less favored, e.g. double WD mergers may lead to accretion-induced collapses rather than to SNe Ia (Hillebrandt & Niemeyer 2000), it is premature to exclude the channel at present since there exists evidence that the channel may contribute to a few SNe Ia (Howell et al. 2006; Branch 2006; Quimby, Höflich & Wheeler 2007; Hicken et al. 2007; Yuan et al. 2007). At present, the single-degenerate Chandrasekhar model is widely accepted, since it is supported by many observations (Parthasarathy et al. 2007)

1.2. Observations

The SD model is supported by many observations. For example, variable circumstellar absorption lines were observed in the spectra of SN Ia 2006X (Patat et al. 2007), which indicates the SD nature of its precursor. Patat et al. (2007) suggested that the progenitor of SN 2006X is a WD + RG system based on the expansion velocity of the circumstellar material, while Hachisu et al. (2008) argued a WD + MS nature for this SN Ia. Recently, two twins of SN 2006X were also reported (Blondin et al. 2009; Simon et al. 2009), and the birth rate and age of the 2006X-like supernovae may be well explained by the WD + MS model

(Meng, Yang & Geng 2009a). Voss & Nelemans (2008) suggested that SN 2007on is also possibly from a WD + MS channel. Moreover, several SD systems are possible progenitors of SN Ia. For example, supersoft X-ray sources (SSSs) were suggested as good candidates for the progenitors of SNe Ia (Livio 1996; Kahabka & van den Heuvel 1997; Hachisu & Kato 2003a,b). Some of the SSSs are WD + MS systems and some are WD + RG systems (Di Stefano & Kong 2003). A direct way to confirm the progenitor model is to search for the companion stars of SNe Ia in their remnants. The discovery of the potential companion of Tycho’s supernova may have verified the reliability of the WD + MS model (Ruiz-Lapuente et al. 2004; Branch 2004; Ihara et al. 2007; Hernández et al. 2009).

Measuring the delay time of SNe Ia (DD, between the episode of star formation producing progenitor systems and the occurrence of SNe Ia) is a very important way to constrain the progenitor system. Although the DD of most of SNe Ia is between 0.3-2 Gyr (Schawinski 2009), there are still SNe Ia with long delay times (older than 10 Gyr inferred from SNe Ia in elliptical galaxies in the local universe, Mannucci et al. 2005) or extremely short delay times (shorter than 0.1-0.3 Gyr, Mannucci et al. 2006; Schawinski 2009; Raskin 2009). Some observational results, i.e. the strong enhancement of the SN Ia birthrate in radio-loud early-type galaxies, the strong dependence of the SN Ia birthrate on the colors of the host galaxies, and the evolution of the SN Ia birthrate with redshift (Della Valle et al. 2005; Mannucci et al. 2005, 2006), may indicate a bimodal distribution of delay time (DDT), in which a part of the SNe Ia explode soon after starburst with a delay time less than 0.1-0.3 Gyr (‘prompt’ SNe Ia), while the rests have a much wider distribution with a delay time of about 3 Gyr (‘tardy’ SNe Ia Mannucci et al. 2006). 10% (weak bimodality) to 50% (strong bimodality) of all SNe Ia belong to the prompt SNe Ia (Mannucci 2008). Whether this is due to the presence of two different channels of explosion (such as single- and double-degenerate) or to a bimodal distribution of some parameter of the exploding systems (such as the mass ratio between the two stars of the binary system) is still unclear.

1.3. Situations

Many works have concentrated on the SD model. To explain prompt SNe Ia, various models were designed. Hachisu et al. (2008) introduced a mass-stripping effect on a main-sequence (MS) or slightly evolved companion star by winds from a mass-accreting white dwarf (Hachisu et al. 1996). Wang et al. (2009a,b) investigated WD + He star channel which can explain SNe Ia with short delay times very well. Lü et al. (2009) even designed a symbiotic channel by assuming an aspherical stellar wind with an equatorial disk. For the tardy SNe Ia, most of works focus on the WD + MS and WD + RG channel. Some authors (Hachisu et al. 1999a,b, 2008; Nomoto et al. 1999, 2003) have studied the SD channel by a simple analytical method to treat binary interactions. Such analytic prescriptions may not describe some mass-transfer phases, especially those occurring on a thermal time-scale (Langer et al. 2000). Li & van den Heuvel (1997) studied the SD from detailed binary evolution calculation, while they considered two WD masses (1.0 and 1.2 M_{\odot}). Langer et al. (2000) investigated the channel for metallicities $Z = 0.001$ and 0.02, but they only studied the case A evolution (mass transfer during core hydrogen burning phase). Han & Podsiadlowski (2004) carried out a detailed study of this channel including case A and early case B (mass transfer occurs at Hertzsprung gap, HG) for $Z = 0.02$. Following the study of Han & Podsiadlowski (2004), Meng, Chen & Han (2009) studied the WD + MS channel comprehensively and systematically at various Z . Based on the works above, WD + MS channel is a very important channel to produce SNe Ia, but the channel may only account for about 1/3 SNe Ia observed and the delay time for the channel is between 0.2-2 Gyr (Han & Podsiadlowski 2004; Meng, Chen & Han 2009). Recently, Xu & Li (2009) proposed a WD + MS model with a thermal unstable accretion disk, which can also produce SNe Ia with long delay time. Although WD + RG channel has been widely studied, it should be investigated carefully by detailed binary evolution calculations with the latest input physics since either the studies are based on a simple analytical method or focus on some special WD masses. In this paper, we want to construct a complete model, which includes WD + MS and

WD + RG channels.

In Section 2, we describe binary evolution model, and present the calculation results in Section 3. We describe our binary population synthesis (BPS) method in Section 4 and show the BPS results in Section 5. We give discussions in Section 6 and summarize our main conclusions in Section 7.

2. BINARY EVOLUTION CALCULATION

2.1. Physical Input

We use the stellar evolution code of Eggleton (1971, 1972, 1973) to calculate the binary evolutions of SD systems. The code has been updated with the latest input physics over the last three decades (Han, Podsiadlowski & Eggleton 1994; Pols et al. 1995, 1998). Roche lobe overflow (RLOF) is treated within the code described by Han et al. (2000). We set the ratio of mixing length to local pressure scale height, $\alpha = l/H_p$, to 2.0, and set the convective overshooting parameter, δ_{OV} , to 0.12 (Pols et al. 1997; Schröder et al. 1997), which roughly corresponds to an overshooting length of $0.25H_p$. The solar metallicity is adopted here ($Z = 0.02$). The opacity table for the metallicity is compiled by Chen & Tout (2007) from Iglesias & Rogers (1996) and Alexander & Ferguson (1994).

2.2. Accretion Disk & Accretion Rates

In an initial binary system, the companion fills its Roche lobe at MS or during HG or RG, and mass transfer occurs. If the mass transfer is dynamically stable, the transferred material forms a disk surrounding the WD. If the effective temperature in the disk is higher than the hydrogen ionization temperature (~ 6500 K), the disk is thermally stable, otherwise an unstable disk is expected (Osaki 1996; van Paradus 1996). This corresponds to a critical mass-transfer rate, below which the disk becomes unstable. The critical mass-transfer rate depends on the orbital period of binary system:

$$\dot{M}_{c,th} = 4.3 \times 10^{-9} \left(\frac{P_{orb}}{4hr}\right)^{1.7} M_{\odot}yr^{-1}, \quad (1)$$

where P_{orb} is the orbital period unit in hour (Osaki 1996; van Paradus 1996). When mass-transfer

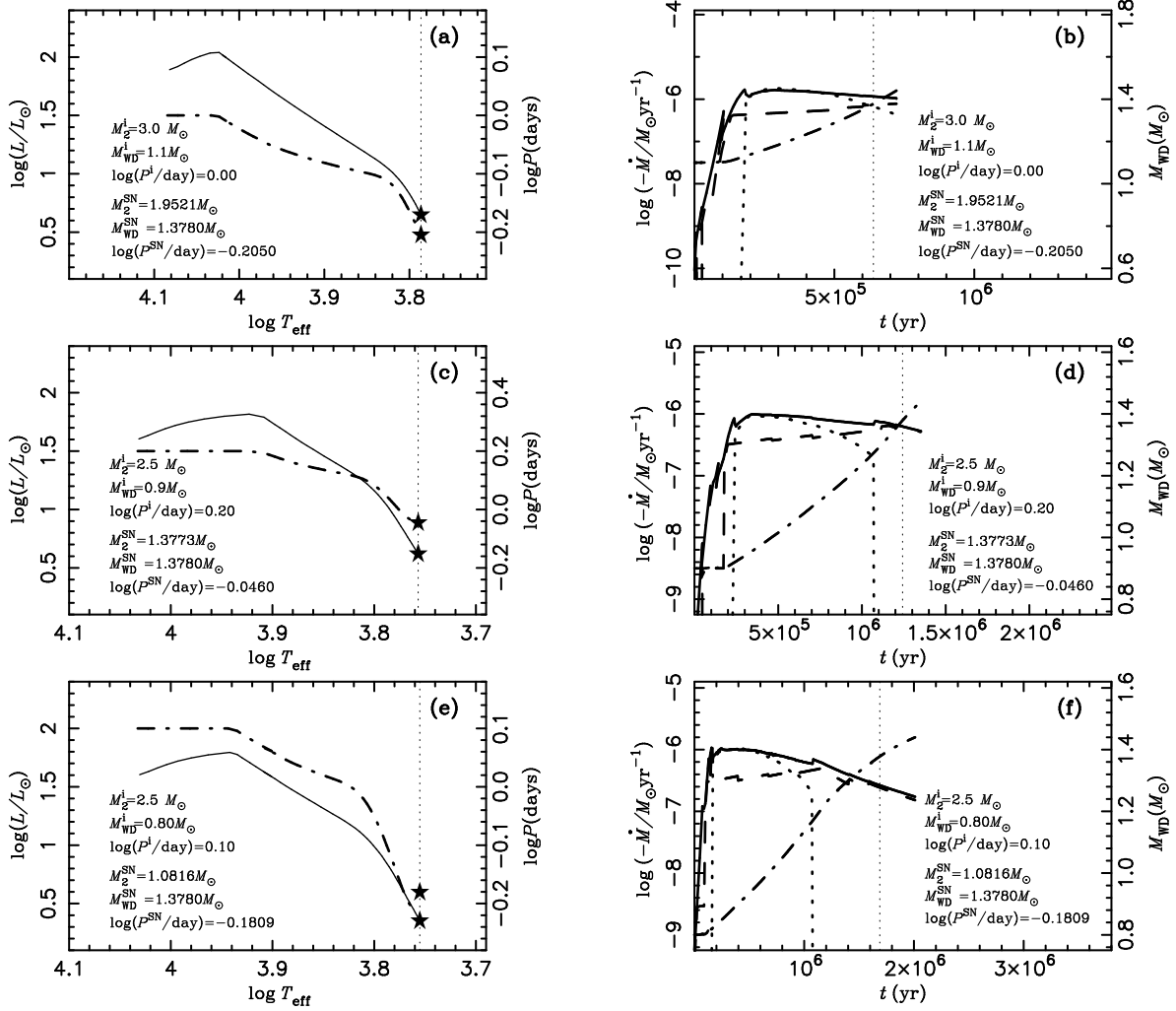


Fig. 1.— Three representative examples of binary evolution calculations. The solid, dashed, dash-dotted and dotted curves show the mass-transfer rate, \dot{M}_{tr} , the mass-growth rate of the CO WD, \dot{M}_{WD} , the mass of the CO WD, M_{WD} , and stripping-off mass-lose rate from secondary, \dot{M}_{strip} , respectively, in panels (b), (d) and (f). Dotted vertical lines in all panels and asterisks in panels (a), (c) and (e) represent the position where the WD is expected to explode as a SN Ia.

rate $|\dot{M}_{\text{tr}}|$ exceeds the critical value, $\dot{M}_{\text{c,th}}$, we assume the accretion disk is stable and the WD accretes the transferred material smoothly at a rate $\dot{M}_{\text{a}} = |\dot{M}_{\text{tr}}|$. If $|\dot{M}_{\text{tr}}|$ is lower than $\dot{M}_{\text{c,th}}$, mass is stored within the disk and no material is accreted by WD. When the materials stored in the disk reaches some critical amount, they are suddenly accreted onto the WD at a rate $\dot{M}_{\text{a}} = |\dot{M}_{\text{tr}}|/d$ due to thermal instability, which may explain dwarf-nova outburst excellently (see the review by Osaki 1996 for details about the disk-instability model). Here, d is duty cycle and is set to be 0.01 as did by Xu & Li (2009). Then, the accretion rate of WD is

$$\dot{M}_{\text{a}} = \begin{cases} |\dot{M}_{\text{tr}}|, & |\dot{M}_{\text{tr}}| \geq \dot{M}_{\text{c,th}}, \\ |\dot{M}_{\text{tr}}|/d, & |\dot{M}_{\text{tr}}| < \dot{M}_{\text{c,th}}, \end{cases} \quad (2)$$

where the typical timescale for the second accretion rate (in the case of the duty cycle) is equal to $M_{\text{disk}}/\dot{M}_{\text{a}}$, where M_{disk} is the mass accumulated in the disk (see review by Lasota (2001) in details).

2.3. WD Mass Growth

Instead of solving stellar structure equations of a WD, we adopt the prescription of Hachisu et al. (1999a) and Hachisu et al. (2008) on WDs accreting hydrogen-rich material from their companions. The following is a brief introduction of this prescription. If WD accretion rate, \dot{M}_{a} , exceeds another critical value, $\dot{M}_{\text{c,H}}$, we assume that a part of accreted hydrogen steadily burns on the surface of WD and is converted into helium at the rate of $\dot{M}_{\text{c,H}}$. The unprocessed matter is assumed to be lost from the system as an optically thick wind at a rate of $\dot{M}_{\text{wind}} = \dot{M}_{\text{a}} - \dot{M}_{\text{c,H}}$ (Hachisu et al. 1996). The optically thick wind may compact into the envelope of WD companion and strips off some hydrogen-rich material from the companion surface. The mass-stripping effect may attenuates the mass-transfer rate from the companion to the WD, and was successfully adapted to explain some quasi-regular SSSs (Hachisu & Kato 2003a,b). The mass-lose rate for the mass-stripping effect, \dot{M}_{strip} is proportional to \dot{M}_{wind} :

$$\dot{M}_{\text{strip}} = c_1 \dot{M}_{\text{wind}}, \quad (3)$$

where c_1 a constant. At present, the value of c_1 is very uncertain. To explain the position of a SSS (V Sge) in the initial orbital period-secondary mass ($\log P^i, M_2^i$) plane, c_1 should be

larger than 0 (Hachisu et al. 2008). Hachisu et al. (2008) checked the influence of c_1 on the donor mass range and found that the range increases with c_1 . Considering primordial primary is more massive than primordial secondary, the c_1 should be smaller 3 (see Fig. 3 in Hachisu et al. 2008 and the discussion in Section 5.1). In this paper, we assume rather arbitrarily that $c_1 = 1.5$, which is the intermediate value between 0 and 3. Then, the mass-lose rate of the companion is $\dot{M}_2 = \dot{M}_{\text{tr}} - \dot{M}_{\text{strip}}$ ¹. The material lost from the system may form circumstellar material (CSM), which is a possible origin of color excess of SNe Ia (Meng et al. 2009).

The critical accretion rate is

$$\dot{M}_{\text{c,H}} = 5.3 \times 10^{-7} \frac{(1.7 - X)}{X} (M_{\text{WD}} - 0.4) M_{\odot} \text{yr}^{-1}, \quad (4)$$

where X is hydrogen mass fraction and M_{WD} is the mass of the accreting WD (mass is in M_{\odot} and mass-accretion rate is in M_{\odot}/yr , Hachisu et al. 1999a).

The following assumptions are adopted when \dot{M}_{a} is smaller than $\dot{M}_{\text{c,H}}$. (1) When \dot{M}_{a} is higher than $\frac{1}{2}\dot{M}_{\text{c,H}}$, the hydrogen-shell burning is steady and no mass is lost from the system. (2) When \dot{M}_{a} is lower than $\frac{1}{2}\dot{M}_{\text{c,H}}$ but higher than $\frac{1}{8}\dot{M}_{\text{c,H}}$, a very weak shell flash is triggered but no mass is lost from the system. (3) When \dot{M}_{a} is lower than $\frac{1}{8}\dot{M}_{\text{c,H}}$, the hydrogen-shell flash is so strong that no material is accumulated on to the surface of the CO WD². We define the growth rate of the mass of the helium layer under the hydrogen-burning shell as

$$\dot{M}_{\text{He}} = \eta_{\text{H}} \dot{M}_{\text{a}}, \quad (5)$$

where η_{H} is the mass accumulation efficiency for hydrogen burning. According to the assumptions above, the values of η_{H} are:

$$\eta_{\text{H}} = \begin{cases} \dot{M}_{\text{c,H}}/\dot{M}_{\text{a}}, & \dot{M}_{\text{a}} > \dot{M}_{\text{c,H}}, \\ 1, & \dot{M}_{\text{c,H}} \geq \dot{M}_{\text{a}} \geq \frac{1}{8}\dot{M}_{\text{c,H}}, \\ 0, & \dot{M}_{\text{a}} < \frac{1}{8}\dot{M}_{\text{c,H}}. \end{cases} \quad (6)$$

¹Please note that \dot{M}_2 and \dot{M}_{tr} are negative, while \dot{M}_{strip} is positive.

²Actually, when a WD undergoes nova explosions, its mass is reduced. However, this should not affect our conclusions about SNe Ia.

Helium is ignited when a certain amount of helium is accumulated. If a He-flash occurs, some of the helium is blown off from the surface of the CO WD. Then, the mass growth rate of the CO WD, \dot{M}_{WD} , is

$$\dot{M}_{\text{WD}} = \eta_{\text{He}} \dot{M}_{\text{He}} = \eta_{\text{He}} \eta_{\text{H}} \dot{M}_{\text{a}}, \quad (7)$$

where η_{He} is the mass accumulation efficiency for helium-shell flashes, and its value is taken from Kato & Hachisu (2004).

We incorporated all the above prescription into Eggleton’s stellar evolution code and followed the evolutions of both the mass donor and the accreting CO WD. The mass lost as optically thick wind is assumed to take away the specific orbital angular momentum of the accreting WD, while the stripped-off material by the optically thick wind is assumed to take away the specific orbital angular momentum of donor star. We calculated about 1600 binary systems, and obtained a large, dense model grid. M_2^i range from $0.6 M_{\odot}$ to $5 M_{\odot}$; the initial masses of CO WDs, M_{WD}^i , from $0.565 M_{\odot}$ to $1.20 M_{\odot}$; the initial orbital periods of binary systems, P^i , from the minimum value (at which a zero-age main-sequence (ZAMS) star fills its Roche lobe) to ~ 80 days. In the calculations, we assume that the WD explodes as a SN Ia when its mass reaches the Chandrasekhar mass limit, i.e. $1.378 M_{\odot}$.

3. BINARY EVOLUTION RESULTS

In Figs. 1 and 2, we present four representative examples and two extreme examples of our binary evolution calculations. The figures show the mass-transfer rate, \dot{M}_{tr} , the growth rate of CO WD, \dot{M}_{WD} , the mass of CO WD, M_{WD} , stripping-off mass-lose rate, \dot{M}_{strip} , the evolutionary track of donor star in the Hertzsprung-Russell (HR) diagram and the evolution of orbital period.

3.1. Case Wind

Panels (a) and (b) in Fig. 1 represent the evolution of a binary system with an initial mass of the donor star of $M_2^i = 3.0 M_{\odot}$, an initial mass of the CO WD of $M_{\text{WD}}^i = 1.10 M_{\odot}$ and an initial orbital period of $\log(P^i/\text{day}) = 0.00$. The donor star fills its Roche lobe at the MS stage which results in a case A RLOF. The mass-transfer rate

exceeds $\dot{M}_{\text{c,H}}$ soon after the onset of the RLOF. This results in a wind phase, where a part of the transferred mass is blown off as an optically thick wind, while the rest is accumulated on to the WD. The optically thick wind collides into the envelope of the companion and strips off some hydrogen-rich material from the surface of the companion. When the mass reaches $M_{\text{WD}}^{\text{SN}} = 1.378 M_{\odot}$, where the WD is assumed to explode as a SN Ia, the system is still in the wind phase (see the thick dotted line). At this point, the mass of the companion is $M_2^{\text{SN}} = 1.9521 M_{\odot}$ and the orbital period is $\log(P^i/\text{day}) = -0.2050$. Since the mass-transfer rate from the secondary continuously exceeds $\dot{M}_{\text{c,H}}$ until the WD explodes as an SN Ia, we call this “Case Wind” as did in Hachisu et al. (2008) and Meng, Yang & Geng (2009b). Case Wind is realized in the region of $2.3 M_{\odot} \leq M_2^i \leq 3.8 M_{\odot}$ and $P^i \leq 5$ days for $M_{\text{WD}}^i = 1.0$ and $1.1 M_{\odot}$. As noticed by Hachisu et al. (2008) and Meng, Yang & Geng (2009b), no Case Wind exists for $M_{\text{WD}}^i < 0.9 M_{\odot}$ (see also Figs. 3 and 4).

Before supernova explosion, Case Wind may be observed as quasi-regular transient SSS such as V Sge (Kato 2009). The hydrogen-rich material lost from the system may form CSM and contribute to the intrinsic color excess of SNe Ia (Meng et al. 2009). The material loses from the system via two ways: as optically thick wind from the surface of WD or stripped-off material by the wind from the companion. The velocity of wind should be larger than the escape velocity of the WD (an order of magnitude of 10^3 km s^{-1}), which is too large to contribute the intrinsic color excess of SNe Ia (Meng et al. 2009). The velocity of the stripped-off material is relatively low ($\sim 100 \text{ km s}^{-1}$, Hachisu et al. 2008). Since the WD explodes during the wind phase, the stripped-off material may form CSM very close the SN Ia and may be the possible origin of supernovae like SN 2002ic and SN 2006X (Hachisu et al. 2008; Meng, Yang & Geng 2009a). It may be helpful for explaining the properties of SNe Ia remnants (Badenes et al. 2007).

3.2. Case Calm

Panels (c) and (d) in Fig. 1 show another example for an initial system with $M_2^i = 2.50 M_{\odot}$, $M_{\text{WD}}^i = 0.90 M_{\odot}$, $\log(P^i/\text{day}) = 0.20$. Similar to the previous example, the companion also fills

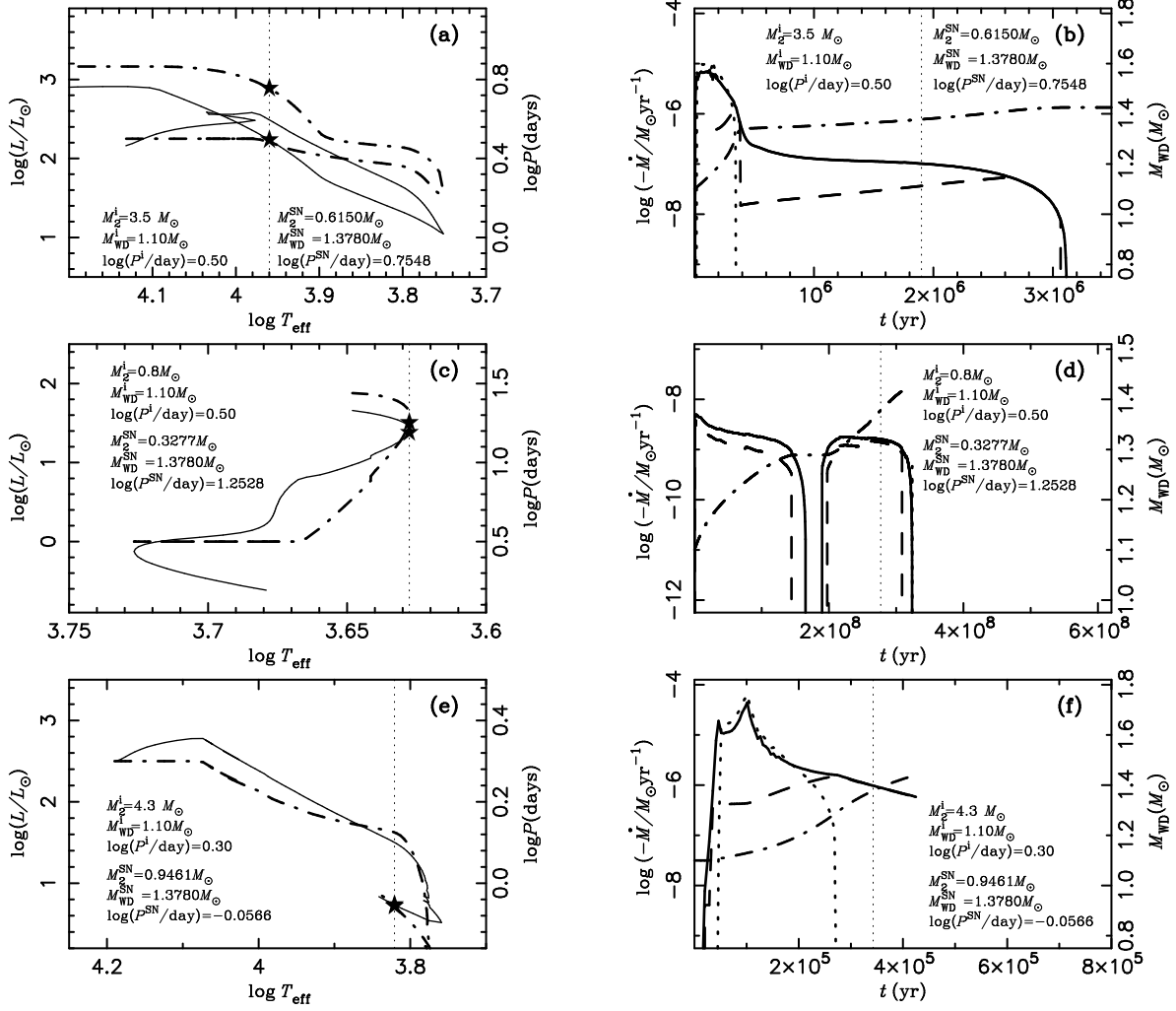


Fig. 2.— Similar to Fig. 1 but for two extreme examples and a WD + RG one.

its Roche lobe at the MS stage and the system experiences a wind phase after the onset of the RLOF. After mass ratio reverse, $|\dot{M}_{\text{tr}}|$ drops until below $\dot{M}_{\text{c,H}}$, but is still higher than $\frac{1}{2}\dot{M}_{\text{c,H}}$, i.e. the optically thick wind stops and hydrogen-shell burning is stable. During this phase, WD reaches $M_{\text{WD}}^{\text{SN}} = 1.378M_{\odot}$, where $M_2^{\text{SN}} = 1.3773M_{\odot}$ and $\log(P^{\text{i}}/\text{day}) = -0.0460$. The main difference between this example and Case Wind is that at the time of the explosion, the system is in the stable hydrogen-burning phase after the optically thick wind phase while Case Wind is still in wind phase. Since WD undergoes steady hydrogen burning at the time of SN Ia explosion, we call this “Case Calm” as did in Hachisu et al. (2008) and Meng, Yang & Geng (2009b). Case Calm can be realized when $M_{\text{WD}}^{\text{i}} \geq 0.80M_{\odot}$ (see also Figs. 3 and 4).

Before supernova explosion, Case Calm may be observed as persistent SSS (Hachisu et al. 2008; Kato 2009). The materials lost as wind or stripped off by the wind form CSM, but they have been dispersed too far to be detected immediately after SN Ia explosion. We even can not expect radio or X-ray emission until at least 10 - 100 yr after the explosion. Then, Case calm would show the properties of “normal” SNe Ia (Branch, Fisher & Nugent 1993; Hachisu et al. 2008).

3.3. Case Nova

The third example in panels (e) and (f) of Fig. 1 represents an initial system with $M_2^{\text{i}} = 2.50M_{\odot}$, $M_{\text{WD}}^{\text{i}} = 0.80M_{\odot}$ and $\log(P^{\text{i}}/\text{day}) = 0.10$. Its evolution is similar to that of Case Calm except that the WD explodes at the phase where $\frac{1}{2}\dot{M}_{\text{c,H}} \geq |\dot{M}_{\text{tr}}| \geq \frac{1}{8}\dot{M}_{\text{c,H}}$. When $M_{\text{WD}}^{\text{SN}} = 1.378M_{\odot}$, $M_2^{\text{SN}} = 1.0816M_{\odot}$ and $\log(P^{\text{i}}/\text{day}) = -0.1809$. Before supernova explosion, hydrogen-burning is unstable, and the system may be observed as a recurrent nova (Hachisu et al. 2008; Kato 2009). Therefore, we call this “Case Nova” as did in Hachisu et al. (2008) and Meng, Yang & Geng (2009b). Case Nova can be realized when $M_{\text{WD}}^{\text{i}} \geq 0.70M_{\odot}$ ³.

³Please note that the WD masses in Figs. 3 and 4 are the initial masses of WDs, while the cases of “Case Wind”, “Case Calm” and “Case Nova” are defined according to the evolutionary stage of a WD binary system at the moment of supernova explosion.

The materials lost as wind or stripped off by the wind form CSM, but they have been dispersed too far to be detected immediately after the SN Ia explosion. It takes at least 100 yr for supernova ejecta to reach the CSM. So, a “normal” SN Ia is expected (Branch, Fisher & Nugent 1993; Hachisu et al. 2008).

3.4. Case DNova

Panels (a) and (b) in Fig. 2 represent the evolution of a binary system with an initial mass of the donor star of $M_2^{\text{i}} = 3.5M_{\odot}$, an initial mass of the CO WD of $M_{\text{WD}}^{\text{i}} = 1.10M_{\odot}$ and an initial orbital period of $\log(P^{\text{i}}/\text{day}) = 0.50$. After RLOF occurs, the system experiences winds phase soon. Then, the system lost much hydrogen-rich material. After mass-ratio reverse, the system experiences the wind, the stable and weakly unstable hydrogen-burning phase one by one, until $|\dot{M}_{\text{tr}}| < \frac{1}{8}\dot{M}_{\text{c,H}}$ and even $|\dot{M}_{\text{tr}}| < \dot{M}_{\text{c,th}}$. At this phase, M_{WD} still does not reach to $1.378M_{\odot}$. Then, the WD increases its mass gradually by accretion from a thermal unstable disk. After about 1.3×10^6 yr, $M_{\text{WD}}^{\text{SN}}$ reaches to $1.378M_{\odot}$, where $M_2^{\text{SN}} = 0.6150M_{\odot}$ and $\log(P^{\text{i}}/\text{day}) = 0.7548$. During this phase, the system may be observed as a dwarf nova (Osaki 1996). So, we call this “Case DNova”. Case DNova is mainly realized when $M_2^{\text{i}}/M_{\text{WD}}^{\text{i}} \gtrsim 3$ and the system is crossing HG at the onset of RLOF. For Case DNova, after $|\dot{M}_{\text{tr}}| < \frac{1}{8}\dot{M}_{\text{c,H}}$, $|\dot{M}_{\text{tr}}|$ may be still higher than $\dot{M}_{\text{c,th}}$. During this phase, the hydrogen-burning is heavily unstable, and then, the system should show the properties of classical nova (Kato 2009).

For the same reason to Case Calm and Case Nova, a “normal” SN Ia is expected for Case DNova.

3.5. Case Instability

Panels (e) and (f) in Fig. 2 illustrate a more extreme case where both the donor and the WD are relatively massive. The initial binary in this case are $M_{\text{WD}}^{\text{i}} = 1.10M_{\odot}$, $M_2^{\text{i}} = 4.3M_{\odot}$ and $\log(P^{\text{i}}/\text{day}) = 0.30$. After about 1×10^5 yr from the onset of RLOF, mass transfer becomes almost dynamically unstable and hence the mass-transfer rate increases sharply, only to drop once the mass ratio has been reversed. When $M_{\text{WD}}^{\text{i}} = 1.378M_{\odot}$, the binary parameters are $M_2^{\text{SN}} = 0.9461M_{\odot}$

and $\log(P^i/\text{day}) = -0.0566$. For a larger initial donor mass, e.g. $M_2^i = 4.5M_\odot$, our calculations show that mass transfer is unstable, and such systems experience a delayed dynamical instability (Hjellming & Webbink 1987; Podsiadlowski et al. 2002). So, we call this case ‘‘Case Instability’’ There are mainly two differences between Case Instability and Case DNova. One is that Case Instability occurs when mass transfer begin at MS stage while Case DNova during HG. The other is that for Case Instability, both the donor and the WD are relatively massive, while Case DNova has no such constraint.

3.6. Case RGB

Panels (c) and (d) in Fig. 2 show a case that RLOF begin at red giant branch (RGB). The parameters of the initial system are $M_{\text{WD}}^i = 1.10M_\odot$, $M_2^i = 0.8M_\odot$ and $\log(P^i/\text{day}) = 0.50$. For the system, the mass transfer rate is always lower than $\dot{M}_{\text{c,H}}$. There is even a broken phase for mass transfer. The WD mainly accretes hydrogen-rich material from a thermal unstable disk. After about 2.7×10^8 yr, $M_{\text{WD}}^{\text{SN}}$ reaches to $1.378M_\odot$, where $M_2^{\text{SN}} = 0.3277M_\odot$ and $\log(P^i/\text{day}) = 1.2528$. To distinguish with Case DNova and due to the RGB nature of the donor, we call this ‘‘Case RGB’’. Case RGB is only realized when $M_{\text{WD}}^i \geq 1.00M_\odot$. In our results, all WD + RG systems explode at the phase of $\dot{M}_{\text{tr}} < \dot{M}_{\text{c,th}}$, and then they should be observed as dwarf nova before SNe Ia.

3.7. Initial Parameters for the Progenitor of SNe Ia

To conveniently compare our results with previous studies in literatures, we summarize the final outcomes of all the binary evolution calculations in the initial orbital period-secondary mass ($\log P^i, M_2^i$) plane. Figs. 3 and 4 summarize the final outcome of our binary evolution calculations in the ($\log P^i, M_2^i$) plane. Filled symbols show the results leading to SNe Ia, where the shape of the symbols indicates the supernova explosions in the optically thick wind phase (filled five-pointed star: $|\dot{M}_{\text{tr}}| > \dot{M}_{\text{c,H}}$), after the wind phase while in the stable hydrogen-burning phase (Filled squares: $\dot{M}_{\text{c,H}} \geq |\dot{M}_{\text{tr}}| \geq \frac{1}{2}\dot{M}_{\text{c,H}}$) or in the unstable hydrogen-shell burning phase (Filled circles: $\frac{1}{2}\dot{M}_{\text{c,H}} > |\dot{M}_{\text{tr}}| \geq \frac{1}{8}\dot{M}_{\text{c,H}}$), and unstable

disk phase (Filled triangles: $|\dot{M}_{\text{tr}}| < \dot{M}_{\text{c,th}}$ and $|\dot{M}_{\text{tr}}|/d \geq \frac{1}{8}\dot{M}_{\text{c,H}}$). Systems experiencing nova explosions and never reaching the Chandrasekhar limit and systems experiencing a dynamical mass transfer are also indicated in the figures.

In Figs. 3 - 5, we also present the contours of the initial parameters in which SNe Ia are expected. In the figures, the left boundaries are determined by the radii of ZAMS stars, i.e. RLOF starts at zero age. the WD + MS systems beyond the right boundaries will undergo dynamically unstable mass transfer at the base of the red giant branch (RGB), while WD + RG systems beyond the right boundaries will experience strong hydrogen-shell flash. The upper boundaries are determined by the delayed dynamical instability or the strong hydrogen-shell flash. The lower boundaries are constrained by the condition that the WD mass accretion rate is larger than $\frac{1}{8}\dot{M}_{\text{c,H}}$ and that the secondaries have enough material to transfer on to CO WDs, which can then increase their masses to $1.378 M_\odot$.

In these figures, we can clearly see that WD + RG channel occurs only when $M_{\text{WD}}^i \geq 1.00M_\odot$ and the region for WD + RG channel increases with initial WD mass and extends to longer period. However, the maximum initial period for WD + RG channel is ~ 25 days, because the mass-transfer rate is very high and most of transferred material loses from system as optically thick wind or stripped-off material if the period is very large. Similar to Xu & Li (2009), the lower boundary of WD + MS channel extends to $\sim 1M_\odot$, because the effect of a thermally unstable disk on the evolution of WD binaries is included in this paper. The upper boundary for WD + MS channel move to $\sim 5M_\odot$, because we include the wind mass-stripping effect suggested by Hachisu et al. (2008). The high donor mass results might contribute to young population of SNe Ia.

In Fig. 5, we overlay the contours for SN Ia production in the ($\log P^i, M_2^i$) plane for initial WD masses of 0.60, 0.70, 0.75, 0.80, 0.90, 1.0, 1.1 and $1.2 M_\odot$. Note that the enclosed region almost vanishes when $M_{\text{WD}}^i = 0.565M_\odot$, which therefore sets the minimum WD mass for which SD model can produce a SN Ia. We wrote the contours leading to SNe Ia into a FORTRAN code, which can be used for population synthesis studies. One can contact X. Meng to request the code.

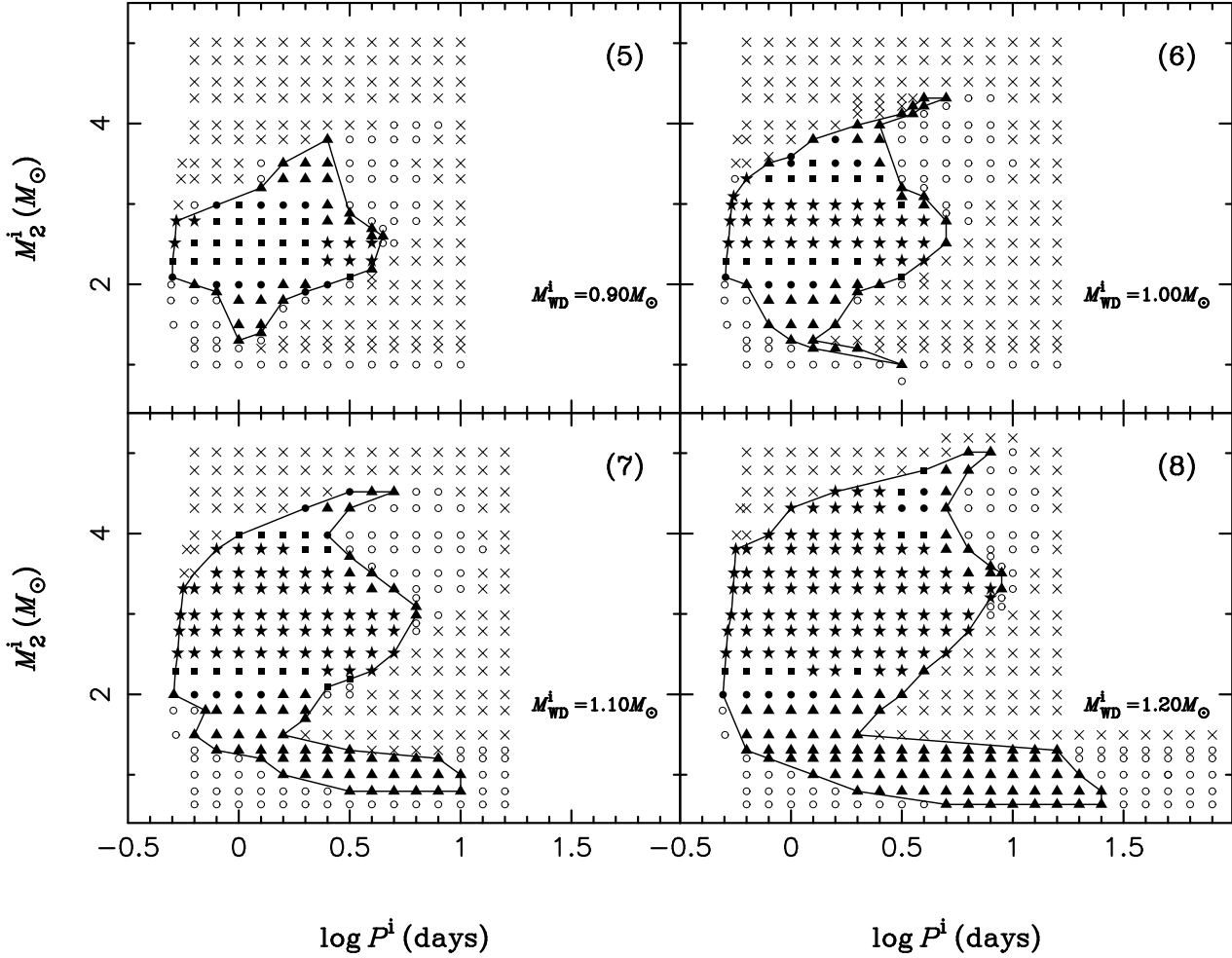


Fig. 3.— Final outcomes of binary evolution calculation in the initial orbital period-secondary mass ($\log P^i, M_2^i$) plane, where P^i is the initial orbital period and M_2^i is the initial mass of donor star (for different initial WD masses as indicated in each panel). Filled five-pointed stars indicate SN Ia explosions during an optically thick wind phase ($|\dot{M}_{\text{tr}}| > \dot{M}_{\text{c,H}}$). Filled squares denote SN Ia explosions after the wind phase, where hydrogen-shell burning is stable ($\dot{M}_{\text{c,H}} \geq |\dot{M}_{\text{tr}}| \geq \frac{1}{2}\dot{M}_{\text{c,H}}$). Filled circles denote SN Ia explosions after the wind phase where hydrogen-shell burning is mildly unstable ($\frac{1}{2}\dot{M}_{\text{c,H}} > |\dot{M}_{\text{tr}}| \geq \frac{1}{8}\dot{M}_{\text{c,H}}$). Filled triangles denote SN Ia explosions during unstable disk phase ($|\dot{M}_{\text{tr}}| < \dot{M}_{\text{c,th}}$ and $|\dot{M}_{\text{tr}}|/d \geq \frac{1}{8}\dot{M}_{\text{c,H}}$). Open circles indicate systems that experience novae explosion, preventing the CO WD from reaching $1.378 M_{\odot}$ ($|\dot{M}_{\text{tr}}| < \dot{M}_{\text{c,th}}$ and $|\dot{M}_{\text{tr}}|/d < \frac{1}{8}\dot{M}_{\text{c,H}}$), while crosses show the systems that are unstable to dynamical mass transfer.

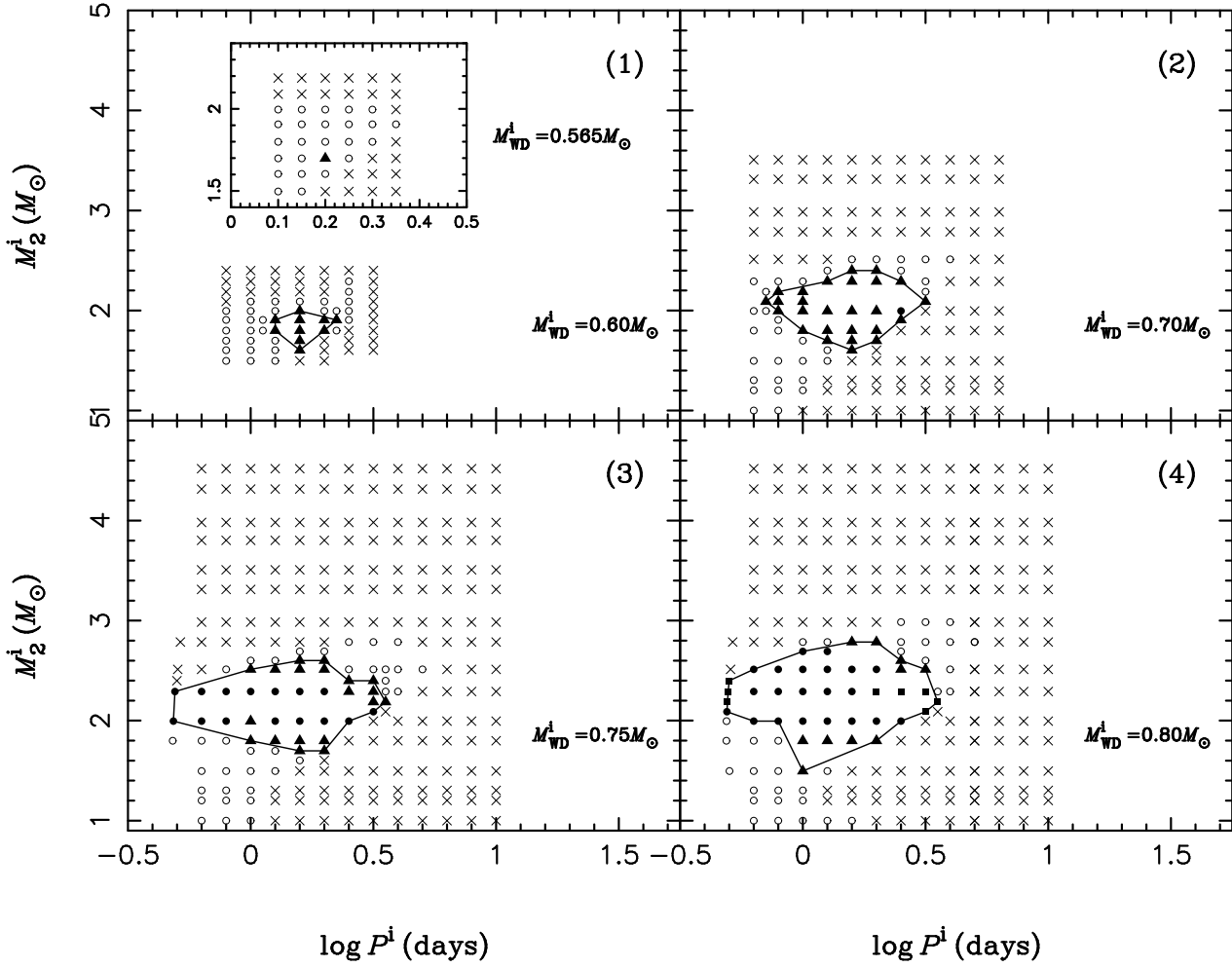


Fig. 4.— Similar to Fig. 3 but for different initial WD masses.

4. BINARY POPULATION SYNTHESIS

Adopting the results in Section 3, we have studied the supernova frequency from the SD channel via the rapid binary evolution code developed by Hurley et al. (2000, 2002). Here after, we use the word *primordial* to represent the binaries before the formation of SD systems and *initial* for SD systems.

4.1. Common Envelope

Common envelope (CE) is very important for the formation of a SD systems. We firstly introduce the treatment for CE in this paper. During binary evolution, the primordial mass ratio (primary to secondary) is crucial for the first mass transfer. If it is larger than a critical mass ratio, q_c , the first mass transfer is dynamically unstable and a CE forms (Paczynski 1976). The ratio q_c varies with the evolutionary state of the primordial primary at the onset of RLOF (Hjellming & Webbink 1987; Webbink 1988; Han et al. 2002; Podsiadlowski et al. 2002; Chen & Han 2008). In this study, we adopt $q_c = 4.0$ when the primary is on MS or crossing HG. This value is supported by detailed binary evolution studies (Han et al. 2000; Chen & Han 2002, 2003). If the primordial primary is on FGB or AGB, we use

$$q_c = [1.67 - x + 2(\frac{M_{cl}^P}{M_1^P})^5]/2.13, \quad (8)$$

where M_{cl}^P is the core mass of primordial primary, and $x = d \ln R_1^P / d \ln M_1^P$ is the mass-radius exponent of primordial primary and varies with composition. If the mass donors (primaries) are naked helium giants, $q_c = 0.748$ based on equation (8) (see Hurley et al. 2002 for details).

Embedded in the CE are the dense core of the primordial primary and the primordial secondary. Due to frictional drag with the envelope, the orbit of the embedded binary decays and a large part of the orbital energy released in the spiral-in process is injected into the envelope (Livio & Soker 1988). Here, we assume that the CE is ejected if

$$\alpha_{CE} \Delta E_{orb} \geq |E_{bind}|, \quad (9)$$

where ΔE_{orb} is the orbital energy released, E_{bind} is the binding energy of common envelope, and α_{CE} is CE ejection efficiency, i.e.

the fraction of the released orbital energy used to eject the CE. Since the thermal energy in the envelope is not incorporated into the binding energy, α_{CE} may be greater than 1 (see Han, Podsiadlowski & Eggleton 1995 for details about the thermal energy). In this paper, we set α_{CE} to 1.0 or 3.0.

4.2. Evolution Channels

There are three channels to produce WD + MS systems according to the situation of the primary in a primordial system at the onset of the first RLOF.

Case 1 (He star channel): the primordial primary is in HG or on RGB at the onset of the first RLOF (i.e. case B evolution defined by Kippenhahn & Weigert 1967). In this case, a CE is formed because of a large mass ratio or a convective envelope of the mass donor. After the CE ejection (if it occurs), the mass donor becomes a helium star and continues to evolve. The helium star likely fills its Roche lobe again after the central helium is exhausted. Since the mass donor is much less massive than before, this RLOF is dynamically stable, resulting in a close CO WD+MS system (see Nomoto et al. 1999, 2003 for details).

Case 2 (EAGB channel): the primordial primary is in early asymptotic giant branch stage (EAGB) (i.e. helium is exhausted in the core, while thermal pulses have not yet started). A CE is formed because of dynamically unstable mass transfer. After the CE is ejected, the orbit decays and the primordial primary becomes a helium red giant (HeRG). The HeRG may fill its Roche lobe and start the second RLOF. Similar to the He star channel, this RLOF is stable and produces WD + MS systems after RLOF.

Case 3 (TPAGB channel): the primordial primary fills its Roche lobe at the thermal pulsing AGB (TPAGB) stage. Similar to the above two channels, a CE is formed during the RLOF. A CO WD + MS binary is produced after CE ejection.

However, only one channel can form WD + RG systems and then produce SNe Ia, i.e. the TPAGB channel. After a WD + MS system is produced from the TPAGB, the companion continues to evolve until RG stage. Then, a WD + RG system forms.

The SD systems continue to evolve and the sec-

ondaries may also fill their Roche lobes at a stage and Roche lobe overflow (RLOF) starts. We assume that if the initial orbital period, P_{orb}^i , and the initial secondary mass, M_2^i , of a SD system locate in the appropriate regions in the $(\log P^i, M_2^i)$ plane for SNe Ia at the onset of RLOF, a SN Ia is then produced.

4.3. Basic Parameters in Monte Carlo Simulation

To investigate the birth rate of SNe Ia, we followed the evolution of 10^7 binaries via Hurley’s rapid binary evolution code (Hurley et al. 2000, 2002). The results of grid calculations in section 3 are incorporated into the code. The primordial binary samples are generated in a Monte Carlo way and a circular orbit is assumed for all binaries. The basic parameters for the simulations are as follows.

(i) The initial mass function (IFM) of Miller & Scalo (1979) is adopted. The primordial primary is generated according to the formula of Eggleton et al. (1989)

$$M_1^{\text{P}} = \frac{0.19X}{(1-X)^{0.75} + 0.032(1-X)^{0.25}}, \quad (10)$$

where X is a random number in the range $[0,1]$ and M_1^{P} is the mass of the primordial primary, which ranges from $0.1 M_{\odot}$ to $100 M_{\odot}$.

(ii) The mass ratio of the primordial components, q , is a very important parameter for binary evolution while its distribution is quite controversial. For simplicity, we take a uniform mass-ratio distribution (Mazeh et al. 1992; Goldberg & Mazeh 1994):

$$n(q) = 1, \quad 0 < q \leq 1, \quad (11)$$

where $q = M_2^{\text{P}}/M_1^{\text{P}}$.

(iii) We assume that all stars are members of binary systems and that the distribution of separations is constant in $\log a$ for wide binaries and falls off smoothly at close separation:

$$an(a) = \begin{cases} \alpha_{\text{sep}}(a/a_0)^m & a \leq a_0; \\ \alpha_{\text{sep}}, & a_0 < a < a_1, \end{cases} \quad (12)$$

where $\alpha_{\text{sep}} \approx 0.070$, $a_0 = 10R_{\odot}$, $a_1 = 5.75 \times 10^6 R_{\odot} = 0.13\text{pc}$ and $m \approx 1.2$. This distribution implies that the numbers of wide binary system per logarithmic interval are equal, and that

approximately 50% of the stellar systems are binary systems with orbital periods less than 100 yr (Han, Podsiadlowski & Eggleton 1995).

(iv) We simply assume a single starburst (i.e. $10^{11}M_{\odot}$ in stars are produced one time) or a constant star formation rate S (SFR) over the last 15 Gyr. The constant SFR is calibrated so that one binary with $M_1 > 0.8M_{\odot}$ is born in the Galaxy each year (see Iben & Tutukov 1984; Han, Podsiadlowski & Eggleton 1995; Hurley et al. 2002). From this calibration, we can get $S = 5 M_{\odot} \text{ yr}^{-1}$ (see also Willems & Kolb 2004). The constant star formation rate is consistent with the estimation of Timmes et al. (1997), which successfully reproduces the ^{26}Al 1.809-MeV gamma-ray line and the core-collapse supernova rate in the Galaxy (Timmes et al. 1997). Actually, a galaxy would have a complicated star formation history, while the two choices here are extremes for simplicity. A constant SFR is a good approximation for spiral galaxies like Galaxy (Rocha-Pinto et al. 2000a,b), while a single starburst is for elliptical galaxies.

5. The RESULTS of BINARY POPULATION SYNTHESIS

5.1. the Birth rates of SNe Ia

Fig. 6 shows Galactic birth rates of SNe Ia for the SD channel. The simulations give a Galactic birth rate of $2.25 - 2.6 \times 10^{-3} \text{ yr}^{-1}$ (thick lines), only slightly lower than the birth rate inferred observationally ($3-4 \times 10^{-3} \text{ yr}^{-1}$, van den Bergh & Tammann 1991; Cappellaro & Turatto 1997). If WD + He star channel is included (Wang et al. 2009b), the Galactic birth rates of SNe Ia for the SD channel becomes $2.55 - 2.9 \times 10^{-3} \text{ yr}^{-1}$ (thin lines). The WD + He star channel contributes to SNe Ia by about 10 per cent.

Fig. 7 displays the evolution of birth rates of SNe Ia for a single starburst of $10^{11} M_{\odot}$. Most of the supernova explosions occur between 0.15 and 2.5 Gyr after the burst, which may mean that S/S0 galaxies with ages below 3 Gyr have a higher SNe Ia birth rate than those older galaxies (see observational results from Gallagher et al. 2008). Similar to Han & Podsiadlowski (2004), we also found that a high α_{CE} leads to a systematically later explosion time, because a high α_{CE} leads to wider WD binaries, and, as a consequence, it takes a

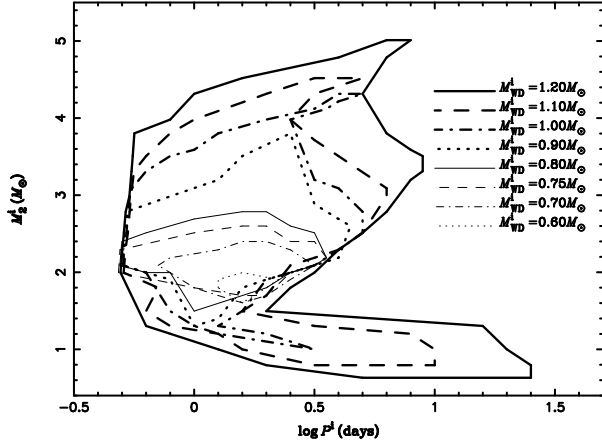


Fig. 5.— Regions in the initial orbital period-secondary mass plane ($\log P^i, M_2^i$) for WD binaries producing SNe Ia for initial WD masses of 0.60, 0.70, 0.75, 0.80, 0.90, 1.00, 1.10 and 1.20 M_\odot . Since the region almost vanishes for $M_{\text{WD}}^i = 0.565M_\odot$, we do not show it in the figure.

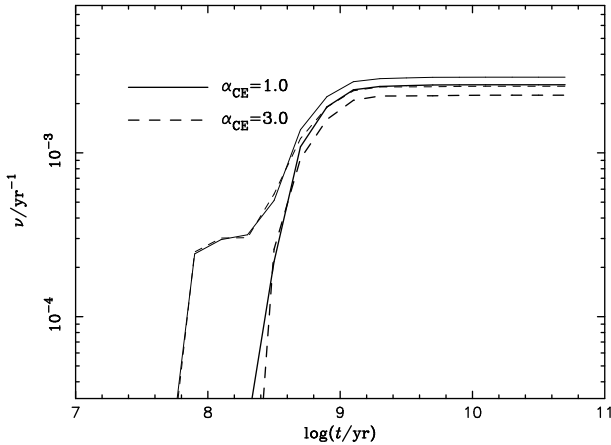


Fig. 6.— The evolution of the birth rates of SNe Ia for a constant star formation rate ($Z=0.02$, $\text{SFR}=5M_\odot\text{yr}^{-1}$). Solid and dashed lines show the cases with $\alpha_{\text{CE}} = 1.0$ and $\alpha_{\text{CE}} = 3.0$, respectively. The thick lines are the results in this paper, while the thin lines are the results including the WD + He star channel from Wang et al. (2009b).

longer time for the secondary to evolve to fill its Roche lobe. Actually, because of the low binding energy of the common envelope and a long primordial orbital period, α_{CE} has a remarkable influence on CO + WD systems from the TPAGB channel. Generally, if a CE can be ejected, a low α_{CE} produces a shorter orbital-period WD + MS system, which is more likely to fulfill the conditions for SNe Ia. Therefore, we see obvious contribution from the TPAGB channel when $\alpha_{\text{CE}} = 1.0$, but no contribution from this channel when $\alpha_{\text{CE}} = 3.0$ (see Meng, Chen & Han 2009 for details regarding the influence of α_{CE} on the TPAGB channel).

In Fig. 7, it is clear that there is a high delay-time tail extending to about 15 Gyr, since the WD + RG system is also included in this paper. However, the contribution of WD + RG channel to SNe Ia is much smaller than that of WD + MS channel. The WD + RG channel mainly contributes to SNe Ia with delay time longer than 6 Gyr.

Although Hachisu et al. (2008) claimed that the model with mass-stripping effect may produce very young population of SNe Ia, there is no SNe Ia with delay time shorter than 10^8 yr in our BPS results. This result is determined by binary evolution, i.e. primordial primary must be more massive than primordial secondary. Let us consider a simple example. For a CO WD of $M_{\text{WD}}^i = 1.1 M_\odot$, its progenitor mass is $\sim 6 M_\odot$ (Umeda et al. 1999; Meng et al. 2008). Then, the upper limit of primordial secondary mass for an initial CO WD binary system with $M_{\text{WD}}^i = 1.1 M_\odot$ is $\sim 6 M_\odot$. When primordial primary evolves to TPAGB phase, a CE forms because of dynamically unstable mass transfer. Embedded in the CE are the dense core of the primordial primary and the primordial secondary. However, if the primordial secondary is only slightly less massive than the primordial primary, the CE may obtain enough energy to eject itself even though the orbit of the new binary decays slightly. Then, it is difficult for the system to fulfill the conditions for SNe Ia. On the contrary, because the orbital period of a system with a lower massive secondary must shrink heavily to eject CE, the system may fulfill the condition for SNe Ia more likely. Actually, almost all of the primordial secondaries leading to SN Ia have a mass less than $4.5 M_\odot$ (see Section 5.2.2).

As noted by Wang et al. (2009b), WD + He star channel may contribute to very young pop-

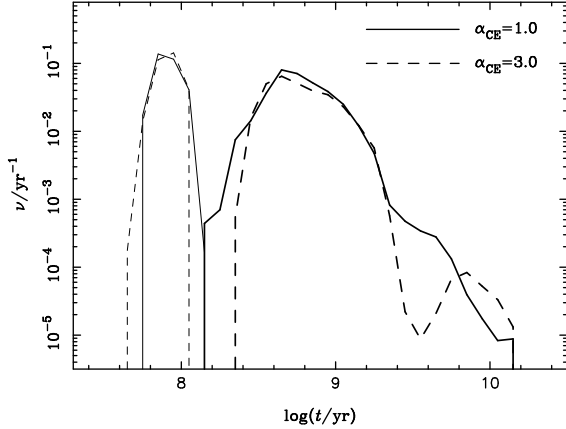


Fig. 7.— The evolution of the birth rates of SNe Ia for a single starburst of $10^{11}M_{\odot}$ for different α_{CE} (solid lines: $\alpha_{\text{CE}} = 1.0$; dashed lines: $\alpha_{\text{CE}} = 3.0$). The thick lines are the results in this paper, while the thin lines are the results from the WD + He star channel from Wang et al. (2009b).

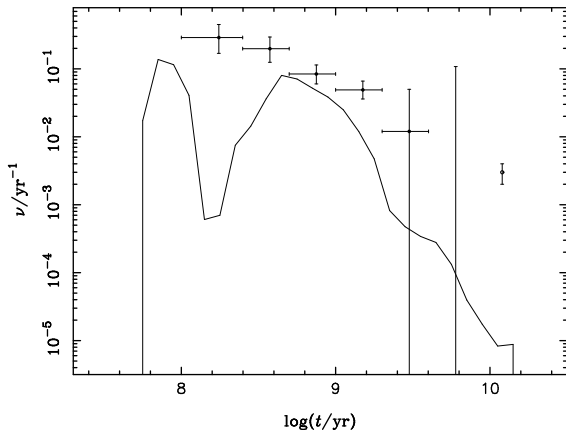


Fig. 8.— The evolution of the birth rates of SNe Ia for a single starburst of $10^{11}M_{\odot}$ for $\alpha_{\text{CE}} = 1.0$ including WD + He star (Wang et al. 2009b), WD + MS and WD + RG channel. The points are from Totani et al. (2008) and the crosses represent error bar.

ulation of SNe Ia, possible all young population. Using the results in this paper and in Wang et al. (2009b), we constructed the evolution of the birth rates of SNe Ia for a single starburst of $10^{11}M_{\odot}$ for $\alpha_{\text{CE}} = 1.0$, shown in Fig. 8. The constructed distribution of delay time (DDT) is much similar to that derived from observations by Mannucci et al. (2006), except that the peak value of young population is smaller than that in Mannucci et al. (2006). The WD + He star channel produces 10 per cent of all SNe Ia, which is the weak bimodality as suggested by Mannucci (2008). In the figure, we also showed the observational results from Totani et al. (2008). The results in this paper seem to be slightly smaller than those in Totani et al. (2008). However, considering the large error of observation in Totani et al. (2008), our results are not inconsistent with observations at least.

5.2. Distribution of Initial Parameters of SD Systems for SNe Ia

Observationally, some SD systems are possible progenitors of SNe Ia (see the review of Parthasarathy et al. 2007). Further studies are necessary to finally confirm them (from both observations and theories). In this section, we will present some properties of initial SD systems for SNe Ia, which may help us to search for the potential progenitors of SNe Ia in the Galaxy.

5.2.1. Distribution of Initial Masses of WDs

In Fig. 9, we show the evolution of the distribution of the initial WD masses in SD systems for different α_{CE} . We also show the evolution of the upper and lower boundary of the distribution. From the figure, we can see that most of WDs explodes as SNe Ia in 2 Gyr later after starburst, where WD + MS systems are the main contributor. α_{CE} does not significantly affect the evolution of the distribution except for WD + MS systems with age less than 2 Gyr. As shown in Meng, Chen & Han (2009), a high α_{CE} , i.e. $\alpha_{\text{CE}} = 3.0$, leads to the disappearing of the WD + MS system from TPAGB channel. So, we can not see high-mass WDs for $\alpha_{\text{CE}} = 3.0$ when age is less than 2 Gyr. For the case of $\alpha_{\text{CE}} = 3.0$, almost all the high-mass WDs are from WD + RG channel. There is a clear trend that the range of the WD mass decreases with age, while the mean

value of WD mass increases. We will discuss this in the Section 6.

5.2.2. Distribution of Initial Secondary Masses

Fig. 10 presents the evolution of distributions of the initial secondary masses for SNe Ia with different α_{CE} . We also show the evolution of the upper and lower boundary of the distribution in the figure. It is clear that the distributions of the initial orbital period and the evolution of the distribution for different α_{CE} are similar. The upper limit of the secondary mass is $4.5M_{\odot}$, lower than $5M_{\odot}$ obtained from binary evolution calculation, which indicates that the mass-stripping effect can not contribute to the young population of SNe Ia.

5.2.3. Distribution of initial orbital periods

Fig. 11 presents the evolution of distributions of the initial orbital period for SNe Ia for different α_{CE} . We also show the evolution of the upper and lower boundary of the distributions in the figure. It is clear that the distributions of the initial orbital period and the evolution of the distributions for different α_{CE} are similar.

6. DISCUSSIONS

6.1. Comparisons with Previous Studies

Previous studies show that the minimum mass of CO WDs leading to SNe Ia, $M_{\text{WD}}^{\text{min}}$, may be as low as $0.70M_{\odot}$ for $Z = 0.02$ (Langer et al. 2000; Han & Podsiadlowski 2004), and this minimum mass even heavily depends on metallicity (Meng, Chen & Han 2009). In this paper, the minimum mass is as low as $0.565M_{\odot}$, which is much lower than $0.70M_{\odot}$. This is because that the mass-stripping effect and the effect of thermal instable disk are incorporated in our study. Recently, Wang, Li & Han (2009) carried out a series of very similar binary evolution calculation to this paper and obtained some much similar results, especially for the WD + RG channel which are almost the same as those in this paper. In their paper, the minimum mass limit is about $0.61 M_{\odot}$, higher than that in this paper. This difference results from the mass-stripping effect considered in this paper.

In Fig. 12, we show a comparison of the results in this paper with those obtained in

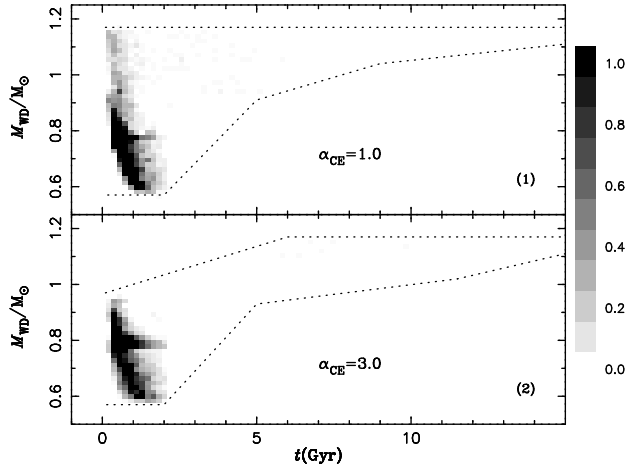


Fig. 9.— The evolution of the distributions of the initial WD masses in SD systems for different α_{CE} , where a single starburst is assumed. The dotted lines shows the evolution of the upper and lower boundary of the distributions.

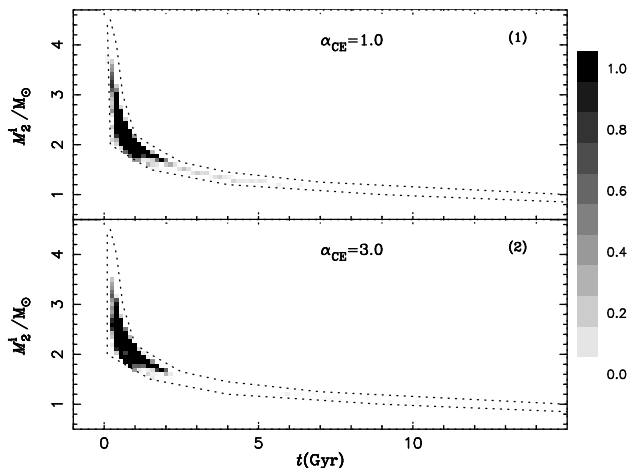


Fig. 10.— The evolution of the distributions of the initial secondary masses in SD systems for different α_{CE} , where a single starburst is assumed. The dotted lines shows the evolution of the upper and lower boundary of the distributions.

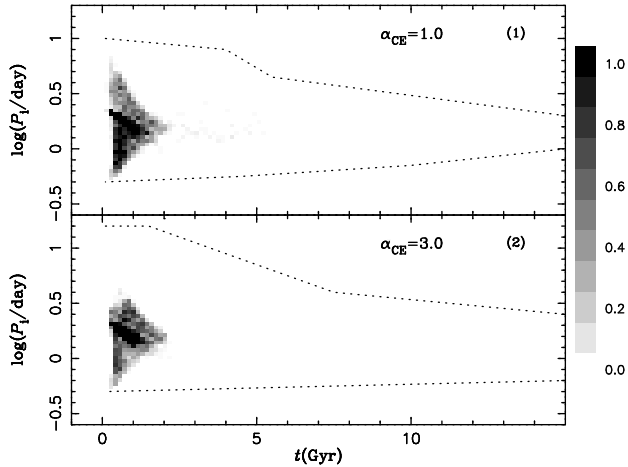


Fig. 11.— The evolution of the distributions of the initial orbital periods in SD systems for different α_{CE} , where a single starburst is assumed. The dotted lines shows the evolution of the upper and lower boundary of the distributions.

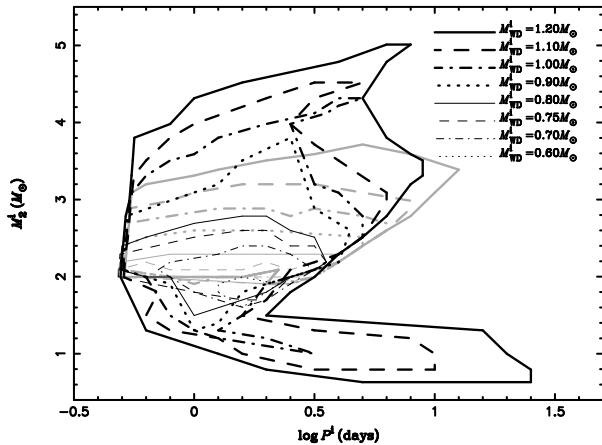


Fig. 12.— A comparison of the results in this paper with those obtained in Meng, Chen & Han (2009). Dark contours show the parameter regions in the $(\log P^i, M_2^i)$ plane for different WD masses that lead to a SN Ia in this paper. The light grey contours are taken from Meng, Chen & Han (2009).

Meng, Chen & Han (2009). Our results are much different from those in Meng, Chen & Han (2009), even only for WD + MS channel. In Meng, Chen & Han (2009), their upper limit for donor stars of $3.7M_{\odot}$ in the progenitor binaries is substantially smaller than the limit of $5.0M_{\odot}$ obtained here, which arises from the mass-stripping effect. The lower limit for donor stars in Meng, Chen & Han (2009) is also much higher than those in this paper, which results from the thermal unstable disk model. The upper limits of donor stars for various initial WD mass in this paper are even higher than those in Wang, Li & Han (2009), which arises from the consideration of the mass-stripping effect in this paper.

In addition, WD + RG channel are also considered in this paper. In our results, there is no WD + RG system with period as long as $10^2 - 10^3$ days as indicated in Li & van den Heuvel (1997) and Nomoto et al. (1999, 2003) (Wang, Li & Han (2009) obtained a similar result to ours). This is because if the period of an initial binary system is too long, the mass transfer rate between WD and donor star is too high and optically thick wind will occur and take much hydrogen-rich material away from the binary system. The donor star then has no enough material to accumulate on to WD.

6.2. Other Possible Channels and Mechanisms for SNe Ia

Fig. 6 shows Galactic birth rates of SNe Ia for the SD channel. The simulations give a Galactic birth rate of $2.55 - 2.9 \times 10^{-3} \text{ yr}^{-1}$ (including WD + He star channel), which is almost consistent with but seems to be slightly lower than the birth rate inferred observationally. Our results are also slightly smaller than those in Totani et al. (2008). In Fig. 13, we compared our results (including WD + He star channel) with the observation from Sullivan et al. (2006). We obtained a similar trend to that in Sullivan et al. (2006), i.e. the birth rate of SNe Ia is proportional to SFR. However, the comparison also shows a slightly lower result than observation, while the example normalized by Galactic birth rates of SNe Ia may be well consistent with the observation in Sullivan et al. (2006). Therefore, there may be other channels or mechanisms contributing to SNe Ia.

Although, the WD + RG system is included here, it is still should be studied carefully in

the future, since this channel may explain some SNe Ia with long delay time. In addition, RS Oph and T CrB (recurrent nova, belonging to WD + RG) are both suggested to be candidates of SNe Ia progenitor (Hachisu et al. 1999b; Hachisu & Kato 2006b; Hachisu et al. 2007), while have a much longer orbital period than those in this paper (Lines, Lines & McFaul 1988; Dobrzycka & Kenyon 1994; Dobrzycka et al. 1996). Perhaps, Symbiotic binaries, consisting of WD and (super)giant, not filling its Roche lobe and having stellar wind should be considered carefully (Branch et al. 1995). Additionally, the progenitor of some SNe Ia (e.g. SN 2006X and SN 2007on) are possible WD + RG systems (Patat et al. 2007; Voss & Nelemans 2008), although WD + MS channel may also be the candidates for the progenitor of the SNe Ia (Hachisu et al. 2008; Meng, Yang & Geng 2009a).

An alternative is the double-degenerate (DD) channel (Iben & Tutukov 1984; Whelan & Iben 1987), although it is theoretically less favored (Hillebrandt & Niemeyer 2000). In this channel, two CO WDs with a total mass larger than the Chandrasekhar mass limit may coalesce and explode as a SN Ia. The birth rate from this channel is comparable to the observational value (Han 1998; Yungelson & Livio 1998, 2000; Tutukov & Yungelson 2002), and SN 2003fg and SN 2005hj likely resulted from the DD channel (Howell et al. 2006; Branch 2006; Quimby, Höflich & Wheeler 2007). Observationally, a large amount of DD systems are discovered (Napiwotzki et al. 2004), but only KPD 1930+2752 is a possible progenitor candidate for a SN Ia via DD channel (Geier et al. 2007). The total mass of KPD 1930+2752 ($\sim 1.52M_{\odot}$) exceeds the Chandrasekhar mass limit and the time scale of coalescence is about 200 Myr estimated from orbital shrinkage caused by gravitational wave radiation (Geier et al. 2007). However, Ergma, Fedorova & Yungelson (2001) argued that, from detailed binary evolution calculation, the final mass of KPD 1930+2752 is smaller than the Chandrasekhar mass limit due to a large amount of mass loss during evolution. In addition, earlier numerical simulations showed that the most probable fate of the coalescence is an accretion-induced collapse and, finally, neutron star formation (see the review by

Hillebrandt & Niemeyer 2000). A definitive conclusion for DD model is thus premature at present, and further studies are needed.

In this paper, we have not considered the influence of rotation on the H-accreting WDs. The calculations by Yoon, Langer & Scheithauer (2004) have shown that the He-shell burning is much less violent when rotation is considered. Then, the He-accretion efficiency may be significantly increase. Meanwhile, the maximum stable mass of a rotating WD may exceed the Chandrasekhar mass limit (i.e. the super-Chandrasekhar mass model: Uenishi et al. 2003; Yoon & Langer 2005; Chen & Li 2009). However, we only focus on the standard Chandrasekhar mass explosions of the accreting WDs in this paper.

Liebert et al. (2003, 2005) and Wickramasinghe & Ferrario (2005) found that about 10% of WDs have magnetic fields higher than 1MG. The mean mass of these WDs is $0.93 M_{\odot}$, compared to mean mass of all WDs which is $0.56 M_{\odot}$ (see the review by Parthasarathy et al. 2007 for details). Thus, the magnetic WDs are more likely to reach the Chandrasekhar mass limit by accretion. Meanwhile, the magnetic field may also affect some properties of WD+MS systems, e.g. the mass transfer rate, the critical accretion rate, the thermonuclear reaction rate etc, leading to a different birth rate of SNe Ia.

6.3. C/O Ratio: the Origin of the Luminosity Scatter of SNe Ia?

It is widely known that there exists a scatter of the maximum luminosity of SNe Ia and the scatter are affected by their environment. The most luminous SNe Ia always occur in spiral galaxies, while both spiral and elliptical galaxies are hosts for dimmer SNe Ia, which lead to a dimmer mean peak brightness in elliptical than in spiral galaxies (Hamuy et al. 1996). In addition, the mean peak brightness of SNe Ia in a galaxy has less variation in the outer regions than in the inner regions (Wang et al. 1997; Riess et al. 1999). To explain these phenomena, Nomoto et al. (1999, 2003) suggested that the ratio of carbon to oxygen (C/O) of an initial CO WD is the origin of the luminosity scatter of SNe Ia. The ratio is a function of WD mass, i.e. a massive CO WD leads to a lower C/O ratio, and thus a lower amount of ^{56}Ni synthesized in the thermonuclear

explosion (Nomoto et al. 1999, 2003), which results in a lower luminosity of SNe Ia (Arnett 1982; Arnett, Branch & Wheeler 1985; Branch 1992). In Fig. 9, we showed the evolution of the range of WD mass with time and found that the range decreases, while the mean mass of CO WD increases with time. If the C/O is the origin of the luminosity scatter of SNe Ia, then our results may well explain the phenomenon found by Hamuy et al. (1996). In a spiral galaxy, because of existing continuous star formation, and then CO WD with various age and initial mass, the spiral galaxy may be host for luminous and dim SNe Ia. However, in an elliptical galaxy, no star formation and no CO WD with young age, only massive CO WD may contribute to SNe Ia, and then a dimmer SNe Ia is expected. The different variation of mean peak brightness of SNe Ia between inner and outer region in a galaxy can also be well explained by the different WD mass resulting from different metallicity (see details in Meng, Chen & Han 2009). So, our results and those in Meng, Chen & Han (2009) uphold the C/O as the origin of the luminosity scatter of SNe Ia. Our results in this paper provide a method to check whether or not the C/O is the origin of the luminosity scatter of SNe Ia. If the C/O is the origin, the elliptical galaxies with age less than 2 Gyr should be hosts of SNe Ia with various luminosity, including very luminous SNe Ia, while older galaxies are only the host of dimmer SNe Ia. In other words, age might be the most important factor to determine the luminosity of SNe Ia, and dimmer SNe Ia would have a wide age distribution. Interestingly, many observations have obtained similar conclusions (Gallagher et al. 2008; Neill 2009; Howell et al. 2009b). Considering the mass of secondary decreases with age (see Fig. 10), a progenitor with more massive secondary should be correlated with more luminous explosion (Howell et al. 2009b). In addition, Howell et al. (2009b) also noticed that low-stretch (dimmer) SNe Ia be evenly distributed between host age older than 5×10^8 yr, which is consistent with our results qualitatively. Our results may also indicate that the mean maximum luminosity of SNe Ia should increase with redshift. Interesting, both Howell et al. (2007) and Sullivan et al. (2009) found that the mean ‘stretch factor’ in-

creases with redshift⁴.

6.4. Young Population of SNe Ia

Observationally, there exists very young SNe Ia (younger than 10^8 yr). To explain these SNe Ia in the frame of SD model, Hachisu et al. (2008) designed a WD + MS channel with mass-stripping effect. However, the detailed BPS study in this paper showed that the WD + MS channel with mass-stripping effect totally can not produce SNe Ia with very short delay time. The WD + He star channel can well produce the young SNe Ia (Wang et al. 2009a,b). The WD + MS, WD + RG and WD + He star channel can produce a weak bimodality of DDT, which might mean that there still exist other channel contributing to the young SNe Ia. Maybe, a symbiotic star with aspherical stellar wind is a possible candidate (Lü et al. 2009).

7. SUMMARY AND CONCLUSIONS

Incorporating mass-stripping effect in Hachisu et al. (2008) and the effect of the instability of accretion disk on the evolution of WD binaries into Eggleton’s stellar evolution code, and including also the prescription of Hachisu et al. (1999a) for mass-accretion of CO WD, We performed binary evolution calculations for more than 1600 close WD binaries. Adopting the results obtained here, we carried out a series BPS study and calculated the birth rate of SNe Ia. We summarize the basic results as following.

1. The detailed binary evolution calculation results further confirmed the suggestion in Hachisu et al. (2008) that the mass-stripping effect may attenuate between WD and the companion, and avoid the formation of a CE, and then increase the donor mass leading to SNe Ia. For a reasonable strength of the mass-stripping effect in physics, i.e. $c_1 = 1.5$, a companion as massive as $5 M_\odot$ can produce an SNe Ia. However, the detailed BPS study show that the upper limit of the companion could be $\sim 4.5 M_\odot$.

2. The detailed binary evolution calculation results confirm that the disk instability could substantially increase the mass-accumulation efficiency

⁴Stretch factor is an indicator of the luminosity of SNe Ia. A luminous SN Ia usually has a higher stretch factor.

for accreting WD, and extend the mass of donor star producing SNe Ia to $\sim 1M_{\odot}$ (see also Xu & Li 2009 and Wang, Li & Han 2009).

3. CO WDs leading to SNe Ia may have a mass as low as $0.565M_{\odot}$.

4. The Galactic birth rate from the SD channel in this paper is $2.25 - 2.6 \times 10^{-3} \text{ yr}^{-1}$, based on α_{CE} . If the WD + He star channel is also included, the Galactic birth rate from the SD channel increases to $2.55 - 2.9 \times 10^{-3} \text{ yr}^{-1}$, only slightly smaller than that derived from observation. Then, there should be other channels or mechanisms contributing to SNe Ia.

5. The DDT from the WD + MS, WD + RG and WD + He star channels may be a weak bimodality. The WD + MS produces most of SNe Ia with delay time between 0.15 – 2.5 Gyr. The WD + RG channel may mainly contribute to SNe Ia with delay time longer than 6 Gyr.

6. The mass-stripping effect may not contribute to very young population of SNe Ia. The WD + He star channel could contribute most of young SNe Ia, even though not all.

7. Our BPS results may uphold the C/O as the origin of the luminosity scatter of SNe Ia and provide a method to verify it.

8. We show the evolution of the initial parameters of SD systems for SNe Ia with time, which is helpful for searching for possible candidates of SNe Ia progenitor systems.

Acknowledgments

This work was supported by Natural Science Foundation of China under Grant Nos. 10963001.

REFERENCES

- Alexander D. R., Ferguson J. W., 1994, *ApJ*, 437, 879
- Arnett W.D., 1982, *ApJ*, 253, 785
- Arnett, W.D., Branch, D., Wheeler, J.C., 1985, *Nature*, 314, 337
- Badenes C., Hughes J.P., Bravo E. et al., 2007, *ApJ*, 662, 472
- Blondin, S., Prieto, J.L., Patat, F., Challis, P., Hicken, M., Kirshner, R.P., Matheson, T., Modjaz, M., 2009, *ApJ*, 693, 207
- Branch D., 1992, *ApJ*, 392, 35
- Branch, D., Fisher, A., Nugent, P., 1993, *AJ*, 106, 2383
- Branch D., Livio M., Yungelson L.R. et al., 1995, *PASP*, 107, 1019
- Branch D., 2004, *Nature*, 431, 1044
- Branch D., 2006, *Nature*, 443, 283
- Cappellaro E., Turatto M., 1997, in Ruiz-Lapuente P., Cannal R.,
- Chen X., Han, Z., 2002, *MNRAS*, 335, 948
- Chen X., Han, Z., 2003, *MNRAS*, 341, 662
- Chen X., Tout C.A., 2007, *ChJAA*, 7, 2, 245
- Chen X., Han, Z., 2008, *MNRAS*, 387, 1416, arXiv: 0804.2294
- Chen, W., Li, X., 2007, *ApJ*, 658, L51
- Chen, W., Li X., 2009, *ApJ*, 702, 686
- Di, Stefano R., Kong, A.K.H., 2003, *ApJ*, 592, 884
- Della Valle, M., Panagia, N., Padovani, P., Cappellaro, E., Mannucci, F., Turatto, M., 2005, *ApJ*, 629, 750
- Dobrzycka, D., & Kenyon, S. J. 1994, *AJ*, 108, 2259
- Dobrzycka, D., Kenyon, S. J., Proga, D., Mikojewska, J., & Wade, R. A. 1996, *AJ*, 111, 2090
- Eggleton P.P., 1971, *MNRAS*, 151, 351
- Eggleton P.P., 1972, *MNRAS*, 156, 361
- Eggleton P.P., 1973, *MNRAS*, 163, 279
- Eggleton P. P., Tout C. A., Fitechett M. J., 1989, *ApJ*, 347, 998
- Ergma E., Fedorova A.V., Yungelson L.R., 2001, *A&A*, 376, L9
- Gallagher, J. S., Garnavich, P. M., Caldwell, N., Kirshner, R. P., Jha, S. W., Li, W., Ganeshalingam, M., Filippenko, A. V., 2008, *ApJ*, 685, 752

- Geier S., Nesslinger S., Heber U., Przybilla N., Napiwotzki R., Kudritzki R.-P., 2007, *A&A*, 464, 299
- Goldberg D., Mazeh T., 1994, *A&A*, 282, 801
- Hachisu, I., Kato, M., Nomoto, K., *ApJ*, 1996, 470, L97
- Hachisu, I., Kato, M., Nomoto, K., Umeda, H., 1999a, *ApJ*, 519, 314
- Hachisu, I., Kato, M., Nomoto, K., 1999b, *ApJ*, 522, 487
- Hachisu I., Kato M., 2003a, *ApJ*, 588, 1003
- Hachisu I., Kato M., 2003b, *ApJ*, 590, 445
- Hachisu I., Kato M., 2006b, *ApJ*, 651, L141
- Hachisu I., Kato M., Luna G.J.M., 2007, *ApJ*, 659, L153
- Hachisu, I., Kato, M., Nomoto, K., 2008, *ApJ*, 679, 1390, (arXiv: 0710.0319)
- Hamuy M., Phillips M.M., Schommer R.A., Schommer R.A., Suntzeff N.B., Maza J., Avilés R., 1996, *AJ*, 112, 2391
- Han Z., Podsiadlowski P., Eggleton P.P., 1994, *MNRAS*, 270, 121
- Han, Z., Podsiadlowski, P., Eggleton, P.P., 1995, *MNRAS*, 272, 800
- Han Z., 1998, *MNRAS*, 296, 1019
- Han Z., Tout C.A., Eggleton P.P., 2000, *MNRAS*, 319, 215
- Han Z., Podsiadlowski Ph., Maxted P. F. L., Marsh T. R., Ivanova N., 2002, *MNRAS*, 336, 449
- Han, Z., Podsiadlowski, Ph., 2004, *MNRAS*, 350, 1301
- Han, Z., Podsiadlowski, Ph., 2006, *MNRAS*, 368, 1095
- Han, Z., 2008, *ApJ*, 677, L109
- Hernández, J.I.G., Ruiz-lapuente, P., Filippenko, A.V., Foley, R.J., Gal-Yam, A., Simon, J.D., 2009, *ApJ*, 691, 1
- Hicken, M., et al. 2007, *ApJ*, 669, L17
- Hillebrandt, W., Niemeyer, J.C., 2000, *ARA&A*, 38, 191
- Hjellming M.S., Webbink R.F., 1987, *ApJ*, 318, 794
- Howell D.A. et al., 2006, *Nature*, 443, 308
- Howell, D.A., Sullivan, M., Conley, A., & Carlberg, R., 2007, *ApJ*, 667, L37
- Howell, D.A. et al., 2009a, arXiv: 0903.1086
- Howell, D.A. et al., 2009b, *ApJ*, 691, 661
- Hurley, J.R., Pols, O.R., Tout, C.A., 2000, *MNRAS*, 315, 543
- Hurley, J.R., Tout, C.A., Pols, O.R., 2002, *MNRAS*, 329, 897
- Hoyle, F. & Fowler, W.A., 1960, *ApJ*, 132, 565
- Iben, I., Tutukov, A.V., 1984, *ApJS*, 54, 335
- Iglesias, C. A., Roger,s F. J., 1996, *ApJ*, 464, 943
- Ihara, Y., Ozaki, J., Doi, M. et al., 2007, *PASJ*, 59, 811, arXiv: 0706.3259
- Kahabka, P. & van den Heuvel, E.P.J., 1997, *ARA&A*, 35, 69
- Kato, M., Hachisu I., 2004, *ApJ*, 613, L129
- Kato, M., 2009, arXiv: 0909.1497
- Kippenhahn, R., Weigert, A., 1967, *ZA*, 65, 251
- Langer, N., Deutschmann, A., Wellstein, S. et al., 2000, *A&A*, 362, 1046
- Lasota, J.-P., 2001, *NewAR*, 45, 449
- Leibundgut, B., 2000, *A&ARv*, 10, 179
- Li, X.D., van den Heuvel, E.P.J., 1997, *A&A*, 322, L9
- Liebert J., Bergeron P., Holberg J.B., 2003, *AJ*, 125, 348
- Liebert J., Bergeron P., Holberg J.B., 2005, *ApJS*, 156, 47
- Lines, H. C., Lines, R. D., & McFaul, T. G. 1988, *AJ*, 95, 1505

- Livio M., Soker N., 1988, ApJ, 329, 764
- Livio M., 1996, LNP, 472, 183
- Livio M., in Truran J., Niemeyer T., eds, Type Ia Supernova: Theory and Cosmology. Cambridge Univ. Press, New York, 1999, p.33
- Lü, G., Zhu, C. Wang, Z., Wang, N., 2009, MNRAS, 396, 1086, arXiv:0903.2636
- Mannucci, F., Della Valle, M., Panagia, N., Cappellaro, E., Cresci, G., Maiolino, R., Petrosian, A., Turatto, M., 2005, A&A, 433, 807
- Mannucci, F., Della Valle, M., Panagia, N., 2006, MNRAS, 370, 773
- Mannucci, F., 2008, ChJAA, 8, 143
- Mazeh T., Goldberg D., Duquennoy A., Mayor M., 1992, ApJ, 401, 265
- Meng X., Chen X., Han Z., 2008, A&A, 487, 625, arXiv: 0710.2397.
- Meng, X., Chen, X., Han, Z., 2009, MNRAS, 395, 2103, arXiv: 0802.2471.
- Meng, X., Chen, X., Han, Z., Yang, W., 2009, RA&A, 9, 1259, arXiv: 0907.2753
- Meng, X., Yang, W., Geng, X., 2009a, NewA, accepted, arXiv: 0910.1915
- Meng, X., Yang, W., Geng, X., 2009b, PASJ, 61, 1251, arXiv: 0908.2470
- Meng, X., Yang, W., 2009, MNRAS, accepted, arXiv: 0909.2167
- Miller G.E., Scalo J.M., 1979, ApJS, 41, 513
- Napiwotzki R., Karl C., Nelemans G. et al., 2004, RMxAC, 20, 113
- Neill, J. D., Sullivan, M., Howell, D. A. et al. 2009, ApJ, in press, arXiv; 0911.0690
- Nomoto, K., Thielemann, F-K., Yokoi, K., 1984, ApJ, 286, 644
- Nomoto, K., Umeda, H., Hachisu, I. Kato, M., Kobayashi, C., Tsujimoto, T., 1999, in Truran J., Niemeyer T., eds, Type Ia Supernova :Theory and Cosmology.Cambridge Univ. Press, New York, p.63
- Nomoto, K., Uenishi, T., Kobayashi, C. Umeda, H., Ohkubo, T., Hachisu, I., Kato, M., 2003, in Hillebrandt W., Leibundgut B., eds, From Twilight to Highlight: The Physics of supernova, ESO/Springer serious “ESO Astrophysics Symposia” Berlin: Springer, p.115
- Osaki, Y., 1996, PASP, 108, 39
- Paczynski B., 1976, in Eggleton P.P., Mitton S., Whelan J., eds, Structure and Evolution of Close Binaries. Kluwer, Dordrecht, p. 75
- Parthasarathy M., Branch D., Jeffery D.J., Baron E., 2007, NewAR, 51, 524, arXiv: 0703415
- Patat, E. et al., 2007, Science, 317, 924
- Podsiadlowski P., Rappaport S., Pfahl, 2002, ApJ, 565, 1107
- Perlmutter, S. et al., 1999, ApJ, 517, 565
- Pols O.R., Tout C.A., Eggleton P.P. et al., 1995, MNRAS, 274, 964
- Pols O.R., Tout C.A., Schröder K.P. et al., 1997, MNRAS, 289, 869
- Pols O.R., Schröder K.P., Hurly J.R. et al., 1998, MNRAS, 298, 525
- Quimby R., P. Höflich, J.C. Wheeler, 2007, ApJ, 666, 1083
- Raskin, C., Scannapieco, E., Rhoads, J., Della Valle, M., 2009, ApJ, arXiv: 0909.4293
- Riess, A. et al., 1998, AJ, 116, 1009
- Riess A. et al., 1999, AJ, 117, 707
- Rocha-Pinto, H.J., Scalo, J., Maciel, W.J., Flynn, C., 2000a, A&A, 358, 869
- Rocha-Pinto, H.J., Scalo, J, Maciel, W. J., Flynn, C., 2000b, ApJ, 531, L115
- Ruiz-Lapuente P. et al., 2004, Nature, 431, 1069
- Schawinski, K., 2009, MNRAS, 397, 717
- Schröder K.P., Pols O.R., Eggleton P.P., 1997, MNRAS, 285, 696
- Simon J. D., Gal-Yam A., Gnat O. et al. 2009, ApJ, 702, 1157

- Sullivan, M. et al. 2006, ApJ, 648, 868
- Sullivan, M., Ellis, R.S., Howell, D.A., Riess, A., Nugent, P.E., Gal-Yam, A., 2009, ApJ, 693, L76
- Timmes F.X., Diehl R., Hartmann D.H., 1997, ApJ, 479, 760
- Tutukov A.V., Yungelson L.R., 2002, Astron. Rep., 46, 667
- Totani T., Morokuma T., Oda T. et al., 2008, PASJ, 60, 1327, arXiv: 0804.0909
- Uenishi T., Nomoto K., Hachisu I., 2003, ApJ, 595, 1094
- Umeda H., Nomoto K., Yamaoka H. et al., 1999, ApJ, 513, 861
- van den Bergh S., Tammann G.A., 1991, ARA&A, 29, 363
- van Paradus, J., 1996, ApJ, 464, L139
- Voss R., & Nelemans G., 2008, Nature, 451, 802
- Wang L., Höflich P., Wheeler J.C., 1997, ApJ, 483, L29
- Wang, B., Meng, X., Chen, X., Han, Z., 2009a, MNRAS, 395, 847
- Wang, B., Chen, X., Meng, X., Han, Z., 2009b, ApJ, 701, 1540
- Wang, B., Li, X., Han, Z., 2009, MNRAS, accepted, arXiv: 0910.2138
- Webbink R. F., 1988, in The Symbiotic Phenomenon, eds. J. Mikolajewska, M. Friedjung, S. J. Kenyon & R. Viotti (Kluwer: Dordrecht), p.311
- Webbink, R.F., 1984, ApJ, 277, 355
- Whelan, J., Iben, I., 1973, ApJ, 186, 1007
- Whelan J., Iben I., 1987, in Philipp A.G.D., Hayes D.S., Liebert J.W., eds, IAU Colloq.95, Second Conference on Faint Blue Stars. Davis Press, Schenectady, p. 445
- Wickramasinghe D.T., Ferrario L., 2005, MNRAS, 356, 1576
- Willems, B., Kolb, U., 2004, A&A, 419, 1057
- Xu, X. & Li, X., 2009, A&A, 495, 243
- Yuan, R.F. et al., 2007, ATEL, 1212
- Yoon, S.-C., Langer, N., Scheithauer, S., 2004, A&A, 425, 217
- Yoon, S.-C., Langer N., 2005, A&A, 435, 967
- Yungelson, L., Livio, M., Tutukou, A. Kenyon, S.J., 1995, ApJ, 447, 656
- Yungelson L., Livio M., 1998, ApJ, 497, 168
- Yungelson L., Livio M., 2000, ApJ, 528, 108

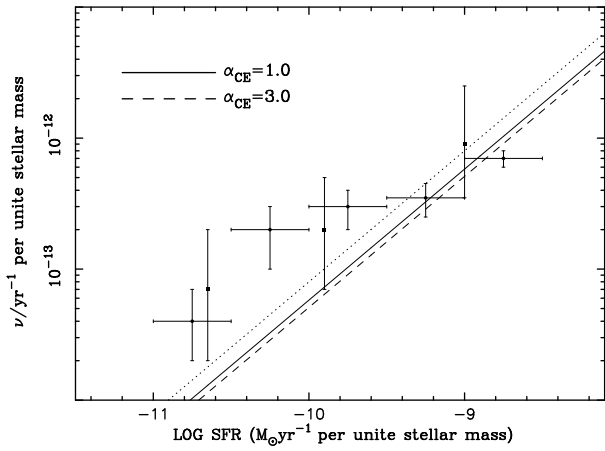


Fig. 13.— SNe Ia rate per unit stellar mass as a function of the SFR per unit stellar mass for various α_{CE} . The WD + He star channel in Wang et al. (2009b) is included. The dotted line represents an example normalized by Galactic birth rates of SNe Ia. The data are obtained from Sullivan et al. (2006) and the cross represent the error bar.